

# Luminescence enhancement in $\text{Eu}^{3+}$ -doped $\alpha$ - and $\gamma$ - $\text{Al}_2\text{O}_3$ produced by pressure-assisted low-temperature combustion synthesis

O. Ozuna and G. A. Hirata<sup>a)</sup>

*Centro de Ciencias de la Materia Condensada, Universidad Nacional Autónoma de México, Apartado Postal 2681, Ensenada, CP 22860, Baja California, México*

J. McKittrick

*University of California at San Diego, Mechanical and Aerospace Engineering and Materials Science and Engineering Program, La Jolla, California 92093-0411*

(Received 15 October 2003; accepted 23 December 2003)

Intense red luminescence in  $\text{Eu}^{3+}$ -doped gamma ( $\gamma$ ) and alpha ( $\alpha$ ) alumina ( $\text{Al}_2\text{O}_3$ ) phosphors obtained by direct and indirect combustion synthesis at low-temperatures is reported.  $\gamma$  and  $\alpha$ - $(\text{Al}_{1-x}\text{Eu}_x)_2\text{O}_3$  are easily produced by combustion synthesis at 280 °C in the range of  $x=0.001$ – $0.06$  at. %. The well-defined direct synthesis allows europium ions to incorporate into the  $\alpha$  or  $\gamma$  alumina lattice in spite of the large size difference between these ions and the aluminum cations in  $\text{Al}_2\text{O}_3$ . These materials yield a strong fluorescence at room temperature due to  $f$ - $f$  transition lines within  $\text{Eu}^{3+}$  ( $4f^6$ ) electron emission configuration. Furthermore, from luminescence measurements, it is deduced that  $\text{Eu}^{3+}$  occupy low-symmetry sites in the  $\text{Al}_2\text{O}_3$  lattice. © 2004 American Institute of Physics. [DOI: 10.1063/1.1650908]

The optical properties of rare-earth (RE) ions in different host materials have been extensively studied for several years. Although there are several reports on this subject, in recent years, considerable attention has been focused on submicrometer/nanometer-sized particles doped with RE ions, since it has been shown that a reduction in particle size often results in an improvement of their structural, electronic, and optical properties.<sup>1</sup>

The interest in RE-doped nanocrystals is fueled by their potential in the fabrication of optical devices, such as optical amplifiers, display phosphors in optoelectronic applications, and microlasers in a submicron dimension.<sup>2,3</sup> This requires that the RE-based nanoparticles be synthesized and integrated with functional substrates, such as single crystals, ceramic microspheres, and nanofibers. It was demonstrated that such materials, especially the ceramics built from nanocrystals, are characterized by pronounced optical properties.<sup>4</sup>

Among the materials investigated to date, few studies have been performed on RE ion-doped aluminum oxide ( $\text{Al}_2\text{O}_3$ ).<sup>5–9</sup> Several structural modifications of  $\text{Al}_2\text{O}_3$  are known with  $\alpha$ - $\text{Al}_2\text{O}_3$ , the only stable phase.  $\alpha$ - $\text{Al}_2\text{O}_3$  is a material with a significant technological importance because of the large optical transparency from an ultraviolet to near-infrared wavelength, excellent mechanical properties, and good chemical stability. Similarly, among the variety of RE ions commonly used to dope different kinds of materials, europium ions ( $\text{Eu}^{3+}$ ) have attracted significant attention because they have tremendous potential for applications as phosphors, electroluminescent devices, optical amplifiers or lasers, and high density optical storage.<sup>1,5,10–13</sup> The emission spectrum of  $\text{Eu}^{3+}$  shows emission lines extending from visible to the near infrared with a relatively simple energy level structure, especially the  ${}^5D_0 \rightarrow {}^7F_J$  ( $J=1,2,3\dots$ ) manifold which enables one to ascertain the microscopic symmetry

around the site, making it an ideal experimental probe of the crystalline environment.

Until recently, this RE-doped  $\alpha$ - $\text{Al}_2\text{O}_3$  materials have only been synthesized by sol-gel techniques, ion-beam implantation, and sonochemical preparation.<sup>5–10</sup> In general, these studies obtained RE-doped transition alumina but have failed in achieving single phase  $\alpha$ - $(\text{Al}_{1-x}\text{Eu}_x)_2\text{O}_3$ . This letter reports the direct and indirect synthesis, morphological characterization, and optical properties of as-synthesized and heat treated  $(\text{Al}_{1-x}\text{Eu}_x)_2\text{O}_3$  ( $x=0.001$ – $0.06$ ) nanocrystalline and submicrocrystalline powder obtained by combustion synthesis technique at a low temperature. This combustion synthesis method is an excellent technique for preparing polycrystalline materials because of its low cost, high yield, and the ability to achieve high-purity single or multiphase complex oxide powders in the as-synthesized state.<sup>14</sup>

In this work,  $\alpha$  and  $\gamma$ - $(\text{Al}_{1-x}\text{Eu}_x)_2\text{O}_3$  powders were synthesized using two preparation methods: A direct and an indirect combustion synthesis. In the direct method, combustion synthesis was carried at atmospheric pressure. In contrast, in the indirect route, the combustion synthesis was carried out in the presence of an additional pressure in the reactor. The reaction is exothermic and occurred at  $\sim 280$  °C (self-ignition temperature).  $(\text{Al}_{1-x}\text{Eu}_x)_2\text{O}_3$  ( $x=0.001$ – $0.060$  at. %) powders were prepared using europium nitrate ( $\text{Eu}(\text{NO}_3)_3 \cdot 6\text{H}_2\text{O}$ ), aluminum nitrate ( $\text{Al}(\text{NO}_3)_3 \cdot 9\text{H}_2\text{O}$ ), and hydrazine ( $\text{N}_2\text{H}_4 \cdot \text{H}_2\text{O}$ ) as a reductive noncarbonaceous fuel that prevents carbon contamination. As soon as the nitrates were dissolved in deionized water, the hydrazine was added. The vessel containing the mixture was introduced into the reactor. A flux of 80 sccm of argon (Ar) was established for 15 min in order to create an inert atmosphere. At this time, the heating process was initiated and the temperature was monitored via a thermocouple system. From this point, two process conditions were used. In the direct process, the Ar pressure was not allowed to build up in the reaction chamber. The chamber was continuously vented with Ar flux.

<sup>a)</sup>Electronic mail: hirata@ccmc.unam.mx

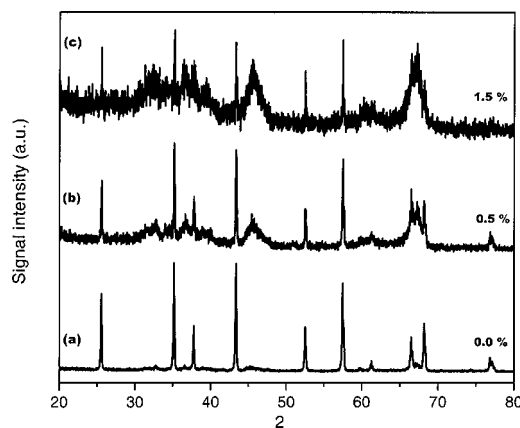


FIG. 1. XRD spectra of  $(\text{Al}_{1-x}\text{Eu}_x)_2\text{O}_3$  obtained through the direct process with different europium concentrations: (a)  $x=0.0\%$ , (b)  $x=0.5$  at. %, and (c)  $x=1.5$  at. %.

Contrarily, in the indirect process, after the first 15 min of Ar flux, the exhaust valve was closed allowing Ar to pressurize the reactor chamber to 0.2 MPa in order to let the reaction take place in this pressurized environment. The pressure inside the reactor was  $\sim 1.3$  MPa just when the reaction started and by the time the reaction was completed (about 1 s), the pressure reached  $\sim 5$  MPa due to the reaction gases.

The phase development in the as-synthesized product and the temperature dependence on the structure formation of the two methods of synthesis, x-ray diffraction (XRD) measurements were carried out using a  $\theta$ - $2\theta$  diffractometer excited with  $\text{Cu } K\alpha I$  ( $\lambda=0.15406$  nm) radiation.

The XRD patterns for the powders of  $(\text{Al}_{1-x}\text{Eu}_x)_2\text{O}_3$  ( $x=0, 0.005, \text{ and } 0.015$  at. %) obtained through the direct process are shown in Fig. 1. From Fig. 1(a), it is clear that through this method, without pressurizing the reactor, it is possible to directly synthesize  $\sim 100\%$  of  $\alpha$ - $\text{Al}_2\text{O}_3$ . The vigorous nature of the reaction is capable of accelerating the kinetics and, therefore, forming  $\alpha$ - $\text{Al}_2\text{O}_3$  without the need for high-temperature treatments, which drastically increase the crystallite size. From Figs. 1(b) and 1(c), it is evident that the combustion synthesis process allows the incorporation of Eu into the  $\alpha$ - $\text{Al}_2\text{O}_3$  lattice despite the large size difference between  $\text{Eu}^{3+}$  ( $\sim 0.9$  Å) and the  $\text{Al}^{3+}$  ( $\sim 0.5$  Å). It is also observed that the presence of the europium ions in the  $\text{Al}_2\text{O}_3$  network inhibits the formation of the  $\alpha$  phase in the as-synthesized state. The prevention of the  $\alpha$ -phase formation is more accentuated when the concentration of the dopant ions is increased.

Figure 2 shows the XRD patterns for the powders of  $(\text{Al}_{0.995}\text{Eu}_{0.005})_2\text{O}_3$  obtained through indirect synthesis (as synthesized and heat treated for 2 h in air at: 1200 °C, 1300 °C, and 1700 °C). Figure 2 helps to elucidate the phase development during heat treatment of the doped powders. It shows that heat treating  $\gamma$ - $(\text{Al}_{1-x}\text{Eu}_x)_2\text{O}_3$  forms  $\theta$ - $(\text{Al}_{1-x}\text{Eu}_x)_2\text{O}_3$ , then  $\alpha$ - $(\text{Al}_{1-x}\text{Eu}_x)_2\text{O}_3$ , and ultimately a mixture of  $\alpha$ - $(\text{Al}_{1-x}\text{Eu}_x)_2\text{O}_3$  and  $\text{AlEuO}_3$ , which implies the crystallization of another phase. It is also observed that the presence of the europium ions retards the formation of the  $\alpha$ -phase to temperatures above 1200 °C. In general, this transformation occurs below 1200 °C for undoped  $\text{Al}_2\text{O}_3$ .<sup>6</sup>

The luminescence properties were investigated by measuring the photoluminescence (PL) spectra of the annealed

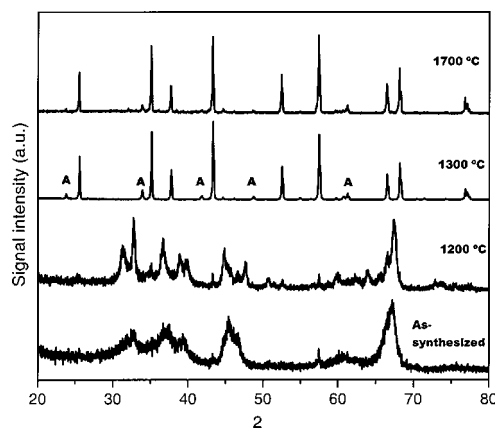


FIG. 2. XRD spectra of  $(\text{Al}_{1-x}\text{Eu}_x)_2\text{O}_3$   $x=0.5\%$  obtained through the indirect process, as synthesized, and heat treated in air for 2 h at various temperatures: 1200 °C, 1300 °C, and 1700 °C. Greek characters represent the various phase transitions of alumina and A indicates the peaks corresponding to  $\text{AlEuO}_3$ .

powders. The PL spectra were recorded using a monochromator (Spex/Triax-180) and detected by a charge coupled device (CCD) camera. The light from a 450 W xenon lamp through the monochromator (Spex/Triax-180) was used for the optical excitation. Figure 3 shows the PL emission spectra, performed at room temperature, of  $(\text{Al}_{1-x}\text{Eu}_x)_2\text{O}_3$  for  $x=0.003$ – $0.040$  samples prepared by the direct method and annealed at 1200 °C for 2 h. The PL spectra of these powders, excited at a wavelength of 395 nm, correspond to the  ${}^7F_0 \rightarrow {}^5L_6$  transition in a direct excitation of the luminescence center. All samples yield intense red emissions around 614 nm. The red emission can be assigned to the hypersensitive  ${}^5D_0 \rightarrow {}^7F_2$  transition using a forced electric dipole transition mechanism, which is a parity forbidden  $f$ - $f$  transition. The peak emission at 594 nm is due to the  ${}^5D_0 \rightarrow {}^7F_1$  magnetic dipole transition and is structurally independent. It can be observed that the samples containing 1.5 and 4.0 at. % of europium show inhomogeneous broad peaks characteristic of  $\text{Eu}^{3+}$  ions occupying a variety of vacant sites in the  $\theta$ - $\text{Al}_2\text{O}_3$  phase. In contrast, the 0.3 at. % sample presents the narrow peaks corresponding to  ${}^5D_0 \rightarrow {}^7F_J$ ,  $J=1, 2, 4$  transitions,  $J=4$  being the most intense emission. This behavior arises from the fact that, at 0.3 at. % of Eu concentration, there are not enough dopant ions to prevent the formation of the  $\alpha$ - $\text{Al}_2\text{O}_3$  at 1200 °C.

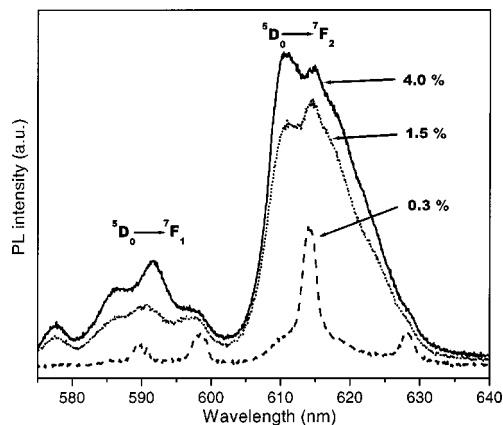


FIG. 3. PL spectra of  $(\text{Al}_{1-x}\text{Eu}_x)_2\text{O}_3$  doped at various concentrations ( $x=0.3, 1.5, \text{ and } 4.0$  at. %).

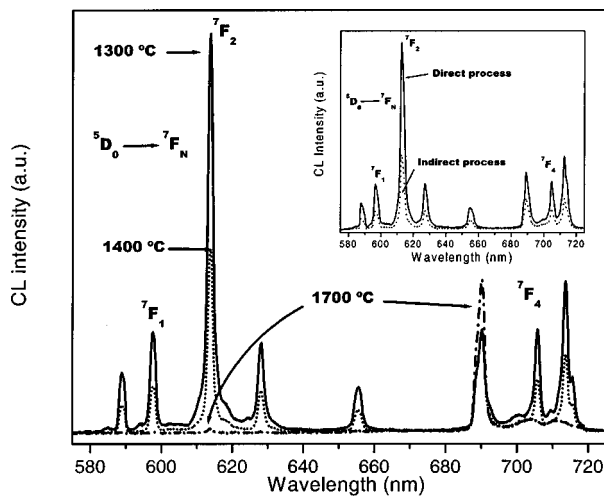


FIG. 4. CL spectra of  $(\text{Al}_{1-x}\text{Eu}_x)_2\text{O}_3$  ( $x=0.5$  at. %) sample heat treated at various temperatures. The inset shows the CL spectra of the  $\text{Eu}^{3+}$  transitions for the samples obtained using the two different synthesis routes.

The cathodoluminescence (CL) emission spectra of the samples were collected using a monochromator (Spex/Triax-180) through an optical fiber and detected by a CCD camera. Figure 4 shows the CL spectra, excited with a 5 keV electron beam of  $(\text{Al}_{0.995}\text{Eu}_{0.005})_2\text{O}_3$  annealed at different temperatures. The spectra consists of a series of well resolved features at 598, 614, and 690 nm, which are assigned to  ${}^5D_0 \rightarrow {}^7F_J$ ,  $J=1, 2, 4$ , transitions, respectively. These emission lines can reveal much about the local environment of the  $\text{Eu}^{3+}$  ion. Among the  ${}^5D_0 \rightarrow {}^7F_J$  transitions, the selection rules make the  ${}^5D_0 \rightarrow {}^7F_1$  and  ${}^5D_0 \rightarrow {}^7F_2$  transitions of particular interest. The emission band at 598 nm, which corresponds to the  ${}^5D_0 \rightarrow {}^7F_1$  transition, is a magnetic dipole transition and hardly varies with the crystal field strength around  $\text{Eu}^{3+}$ . However, the hypersensitive transition  ${}^5D_0 \rightarrow {}^7F_2$  at 614 nm is electric dipole allowed, consequently, it depends on the local electric field and, hence, the local symmetry. From these considerations, it is clear that the  $({}^5D_0 \rightarrow {}^7F_2)/({}^5D_0 \rightarrow {}^7F_1)$  intensity ratio, called the asymmetry ratio, gives a measure of the degree of distortion from the inversion symmetry of the local environment of the  $\text{Eu}^{3+}$  ion lattice. The asymmetry ratio of the  $(\text{Al}_{1-x}\text{Eu}_x)_2\text{O}_3$  sample heat treated at 1300 °C is calculated as 4.0 and for the sample treated at 1400 °C has a value of 3.6. A large value of the asymmetry ratio obtained for both samples are indicative of strong electric fields of low symmetry at the  $\text{Eu}^{3+}$  ions. Both results suggest that  $\text{Eu}^{3+}$  ions occupy low symmetry sites as theoretically inferred by Verdozzi *et al.*<sup>12</sup> It is clear that the asymmetry ratio decreases with an increase of the thermal treatment. For the sample annealed at 1700 °C, the asymmetry ratio is dramatically reduced, to about 1.7, suggesting that the  ${}^5D_0 \rightarrow {}^7F_2$  transition is now strongly forbidden due to a change in the symmetry occupied by most of the  $\text{Eu}^{3+}$  ions. We also observe an increase in the  ${}^5D_0 \rightarrow {}^7F_4$  transition at this temperature of annealing. Depicted in the inset of Fig. 4 is a plot of the CL emission spectra of  $(\text{Al}_{0.995}\text{Eu}_{0.005})_2\text{O}_3$  samples obtained through the two preparation methods and heat treated in air for 2 h at 1300 °C. When compared the CL intensity of the  ${}^5D_0 \rightarrow {}^7F_2$  transition, at 614 nm, the sample prepared by the direct method offers the best performance for CL applications. We believe that the best CL performance

offered by the samples obtained through the direct method is due to the formation of larger crystals of  $\alpha\text{-Al}_2\text{O}_3$ . It is also observed that, independent of the synthesis route, all samples presented an asymmetry ratio of 4.0, which indicates that the  $\text{Eu}^{3+}$  ions occupy a site with no inversion symmetry.

In summary, it is shown that two polycrystalline phases of  $\text{Eu}^{3+}$ -doped alumina,  $\gamma\text{-Al}_2\text{O}_3$  or  $\alpha\text{-Al}_2\text{O}_3$  for  $x=0.001\text{--}0.06$  can be obtained by pressure-assisted low-temperature combustion synthesis. With these methods, it is possible to obtain highly luminescent  $\text{Eu}^{3+}$ -doped  $\text{Al}_2\text{O}_3$  powders at temperatures of  $\sim 280$  °C, that present uniformity and small particle sizes. The initial pressure is the crucial parameter in the controlled synthesis of  $\text{Eu}^{3+}$ -doped  $\gamma\text{-Al}_2\text{O}_3$  or  $\alpha\text{-Al}_2\text{O}_3$  polycrystalline phases. The direct  $(\text{Al}_{1-x}\text{Eu}_x)_2\text{O}_3$  synthesis is an advantageous way, concerning the temperature of the submicrocrystalline formation and the product morphology, which may be the reason for the high CL intensity achieved by this method. Additionally, this well-defined synthesis condition allows europium ions to incorporate easily into the ( $\alpha$  or  $\gamma$ )- $\text{Al}_2\text{O}_3$  lattices in spite of the large size difference between Eu and Al ionic radii. Strong PL in nanocrystalline  $\gamma\text{-Al}_2\text{O}_3:\text{Eu}^{3+}$  excited at  $\lambda=395$  nm and high intensity CL in  $\alpha\text{-Al}_2\text{O}_3:\text{Eu}^{3+}$  phosphors were measured at room temperature due to  $f\text{--}f$  transition lines within  $\text{Eu}^{3+}$  ( $4f^6$ ) electron emission configuration. Furthermore, from the analysis of the luminescence spectra which are revealed by the local environment of the  $\text{Eu}^{3+}$ , it is established that europium ions occupy low symmetry sites in the network structure. These are important criterion for the application of these phosphors in lamps and displays.

The technical assistance of E. Aparicio, M. Sainz, F. Ruiz, J. A. Diaz, A. Tiznado, E. Medina, I. Gradilla, E. Flores, V. Garcia-Gradilla, G. Vilchis, P. Casillas, and J. A. Peralta is gratefully appreciated. The authors would like to acknowledge financial support from CONACYT-Mexico (Grant Nos. 35971-U and 40128-F), DGAPA-UNAM (Grant No. IN105201), Materials Corridor Initiative (Grant No. DE-FC04-01AL67097), University of California Energy Institute and DOE-USA (DE-FC26-01NT41202).

- <sup>1</sup>M. D. Barnes, A. Mehta, T. Thundat, R. N. Bhargava, V. Chabra, and B. Kulkarni, *J. Phys. Chem. B* **104**, 6099 (2000).
- <sup>2</sup>D. K. Williams, B. Bihari, B. M. Tissue, and J. M. McHale, *J. Phys. Chem. B* **102**, 916 (1998).
- <sup>3</sup>A. Polman, *J. Appl. Phys.* **82**, 1 (1997).
- <sup>4</sup>B. N. Bhargava, D. Gallagher, X. Hang, and A. Nurmikko, *Phys. Rev. Lett.* **72**, 416 (1994).
- <sup>5</sup>N. Can, P. D. Townsend, D. E. Hole, H. V. Snelling, J. Ballesteros, and C. N. Afonso, *J. Appl. Phys.* **78**, 6737 (1995).
- <sup>6</sup>A. A. Kaplyanskii, A. B. Kulinkin, A. B. Kutsenko, S. P. Feofilov, R. I. Zakharchenya, and T. N. Vasilevskaya, *Phys. Solid State* **40**, 1310 (1998).
- <sup>7</sup>J. K. Krebs and U. Happek, *J. Lumin.* **94**, 65 (2001).
- <sup>8</sup>A. Pilonnet-Minardi, O. Marty, C. Bovier, C. Garapon, and J. Mugnier, *Opt. Mater. (Amsterdam, Neth.)* **16**, 9 (2001).
- <sup>9</sup>T. Ishizaka, R. Nozaki, and Y. Kurokawa, *J. Phys. Chem. Solids* **63**, 613 (2002).
- <sup>10</sup>A. Gedanken, R. Reisfeld, L. Sominski, Z. Zhong, Y. Kolytyn, G. Panzer, M. Gaft, and H. Minti, *Appl. Phys. Lett.* **77**, 945 (2000).
- <sup>11</sup>M. Nogami, T. Hayakawa, and T. Ishikawa, *Appl. Phys. Lett.* **75**, 3072 (1999).
- <sup>12</sup>C. Verdozzi, D. R. Jennison, P. A. Schultz, M. P. Sears, J. C. Barbour, and B. G. Potter, *Phys. Rev. Lett.* **80**, 5615 (1998).
- <sup>13</sup>G. Blasse and B. C. Grabmaier, *Luminescent Materials* (Springer, Berlin, 1994).
- <sup>14</sup>R. García, G. A. Hirata, and J. McKittrick, *J. Mater. Res.* **16**, 1059 (2001).